Journal of Applied Research in Science and Humanities

Applications of Nanomaterials

Esraa Ahmed, Afnan Abdelhamid, Aya Yehia, Jolia Emad, Madona Faheem, Merna Tawadros, Nancy Mohamed, Noura Galal

Supervisor: Hayam Osman Taha

Associate Professor of Physics

Ain Shams University, Faculty of Education, Program Physics

Abstract

Hydrogen is seen as a highly promising sustainable energy source for the future, especially in applications like transportation. However, the challenge lies in finding efficient materials for its storage, particularly for vehicle fuel. Nanocones have emerged as a potential storage material for hydrogen. In this research, Using Density Functional Theory (DFT), hydrogen adsorption on Ni–doped carbon nanocones (Ni–CNCs) and carbon nanocone sheets (Ni–CNCSs) with inclination angle 120° was examined. The functionalized Ni atom is found to be adsorbed on CNC and CNCS with an adsorption energy of –4.04 and –6.365 eV, respectively. The Ni– functionalized CNC and CNCS bind up to five and three molecules of hydrogen respectively. Where the adsorption energy of the complexes nH_2–Ni–CNC (n=3:5) is –0.573, –0.428 and –0.343 eV, respectively and nH_2–Ni–CNCS (n =2,3) is –0.478 and –0.210 eV, respectively. All of them are inside the Department of Energy domain (–0.2 to –0.6 eV). Gravimetric capabilities are estimated to be 5.05 wt% for CNC and 3.97 wt% for CNCS.

Keywords

Ni–doped; DFT; hydrogen storage; CNCs and CNCSs

1. Introduction: Multiple economies worldwide heavily rely on fossil fuels like coal, oil, and natural gas for industrial growth, urban development, and managing population growth, leading to increased global warming and environmental pollution. There is a necessity for strategies to reduce high carbon emissions and greenhouse gas levels. Renewable energy sources have emerged as a sustainable alternative to traditional fossil fuels, as they produce minimal carbon emissions (Mohsin, 2021,111999).

Renewable energy systems (RESs) have become crucial for meeting the increasing energy demands sustainably and in an eco-friendly manner. However, the intermittent nature of RESs creates challenges for deployment. To address this issue, battery energy storage systems are commonly used in microgrids. However, batteries have restrictions in terms of size, lifespan, and cost, leading to the exploration of hydrogen-based storage systems as an alternative. Hydrogen, a colorless, odorless, flammable gas, is the lightest and most abundant element in the universe, produced from sources like water, natural gas, and biomass. When used as a fuel, hydrogen can be converted into electricity in a hydrogen fuel cell, known for its high efficiency and producing only water and heat as by-products. Despite its numerous advantages, the widespread adoption of hydrogen fuel cells is hindered by high production costs and infrastructure needs. Nevertheless, hydrogen is considered an environmentally friendly fuel that does not release harmful substances when burned at low temperatures(Modu, 2023, 38354).

Various methods are being explored for hydrogen storage and transport, including gaseous or liquid storage, chemical forms of storage, and hydrogen adsorption on carbon nanomaterials (Züttel , 2004, 72).

In recent years, researchers have conducted substantial research into carbon nanotube hydrogen sorption properties. However, there has been much debate about the storage capabilities of several of these materials since the initial study on the potential for room temperature hydrogen storage by carbon nanotubes (Dillon,1997,377).

Carbon allotropes, such as graphene, fullerene, and carbon nanotubes, are considered promising materials for hydrogen storage due to their properties like high surface area, chemical stability, low cost, and strong carbon-hydrogen reactivity. Curved carbon structures like carbon nanocones are also highlighted for their potential as hydrogen adsorbents given that hydrogen can adsorb more readily in the curved areas of carbon nanotubes, carbon nanocones (CNCs).

Additionally, because of its unique structure, CNCs have unique electrical and mechanical qualities that offer hydrogen storage an extra benefit (Kose,2022,108921,0925-9635)

Decoration of carbon-based materials with transition metal atoms like Ti, Ni, Sc, and V is expected to enhance hydrogen storage capabilities and binding energies, offering potential gravimetric density improvements (Abdel Aal,2015, 4).

Advanced density functional theory (DFT) calculations were used to study the impact of a carbon vacancy on hydrogen adsorption onto a Ti-functionalized C_{60} fullerene when H2 is aligned along different axes (Shalabi, 2023,1211).

The study intends to differentiate between reversible and irreversible interactions between hydrogen and Ni-doped C60 fullerene. Specific complexes represent reversible and irreversible interactions within or outside the Department of Energy's (DOE) domain for practical applications (- 0.20 to - 0.60 eV (Shalabi,2014,928754).

Using the (DFT) calculations research examines the ability of Ti-functionalized carbon nanocones and sheets to store hydrogen. Results indicate that both nanocones and sheets could be potential hydrogen storage materials where the average adsorption energies per H_2 molecule (- 0.54 & -0.39 eV), falling within the DOE target range for adsorption energies. These materials have the potential to achieve significant hydrogen storage capacities (Shalabi,2014,19333).

Our research will focus on examining how hydrogen is stored on carbon nanocones (CNCs) that are functionalized with Nickel, as well as carbon nanocone sheets (CNCSs) that have an inclination angle of 120º and a height of 5 Å. We tend to focus our interest on structural parameters, binding energies, hydrogen storage capacity, and electronic properties in configurations. The study is ordered as follows: In Section II, we present the computational model, the results in Section III, the interpretation in Section IV, and the conclusion in Section V.

2. The Computational Methods

Nanotube modular is used to build 36 carbon atoms in a finite-length nanocone and nanocone sheet cluster with a disclination angle of 120°, height of 5 Å, and a C-C bond length of 1.421 Å, with 12 and 10 hexagonal rings, respectively. To avoid dangling bonds, the edge atoms in each cluster have reached saturation with hydrogen (Xu H,2017,37, Tomson, 2019, 478, Soleymanabadi,2013,54). Within density functional theory (DFT), simulations based on the first principle have been conducted to investigate the interactions between Ni and CNC as well as Ni and CNCS. B3LYP (Becke's three-parameter exchange functional(B3)) with Lee, Yang, and part

(LYP) correlation function (Becke,1993,5648 – Lee,1988,785). It is used theoretically to perform the computations in this study. Because it offers a reasonably accurate description of metal interactions and, for magnetic systems, a picture that falls somewhere between the HF (Hartree–Fock) and pure gradient corrected approximation descriptions, the B3LYP hybrid functional has been selected (Martin,1997,1539–De Moreira,2002, 235109). The benefits of using DFT calculations for hydrogen storage materials research can be summarised as the precision of computed thermodynamic values, efficiency relative to experiment, and thermodynamic predictions of new functionalized nanostructures (Wolverton, 2008,064228)

Single–point energy (SPE) computations for NiC_{36} NC and NiC_{36} NCS at the B3LYP/6–31G were then performed using the optimized geometries that were discovered. All computations were performed using the Gaussian 0.9 system. The corresponding Gauss View 5.0 software is used to visualize the optimal geometries (Frisch,2010)

3. Results of Research

We have first considered the structure of CNC and CNCS with a disclination angle of 120° and height of 5 Å ,containing 36 carbon atoms, the relaxed structures, using DFT are illustrated in Figure 1(a, b, c). To reduce boundary effects, the CNC and CNCS were hydrogen–saturated at the ends.

Table 1.

Structural and energetic parameters of the optimized nH_2 –Ni– C_{36}– H_{12}(n=1–5) (cone) systems. All distances (d) are given in Å , energy $\Delta E_{ads.}$, in eV, calculated at the B3LYP/6–31G level of theory.

System	$\Delta E_{ads.}$	d(Ni–C)	d(C–C)	d(Ni–H)	d(H–H)	Wt%
C_{36}– H_{12}	-------	-------	1.463	----------	-----	
Ni– C_{36}– H_{12}	–4.13	2.01	1.492	-------	-----	
$1H_2$– C_{36}– H_{12}	–0.008	-------	-------	4.229, 3.532	-----	
$1H_2$– Ni– C_{36}– H_{12}	–0.813	1.8757	1.547	1.857, 1.604	0.840	
$2H_2$– Ni– C_{36}– H_{12}	–0.847	1.9024 1.9046	1.527	1.595, 1.633 1.594, 1.631	0.814, 0.814	
$3H_2$– Ni– C_{36}– H_{12}	–0.573	1.9048	1.5252	1.6329, 1.5983	0.744, 0.815	

		1.9069		1.6339, 1.5973 2.8300, 3.5310	0.813	
$4H_2$– Ni– C_{36}– H_{12}	–0.428	1.9036 1.9037	1.5266	4.321, 4.824 1.5965, 1.63299 1.6334, 1.59723 3.9595, 3.4724	0.814, 0.744 0.813, 0.743	
$5H_2$– Ni– C_{36}– H_{12}	–0.343	1.9026 1.9024	1.527	4.224, 4.7422 1.5944, 1.636 1.6325, 1.5959 4.131, 3.788 4.429, 4.7822	0.743, 0.743 0.813, 0.813 0.744	5.05

Table 2.

Natural bond orbital charges (Q) in au, HOMO, LUMO, and Eg energies in (eV), ionization potential (I/ eV), electron affinity (A/ eV) and dipole moment (μ) in Debye, for nH_2 –Ni– C_{36}– H_{12}(n=1–5) (cone) systems.

System	Q_{Ni}	Q_C	QH	LUMO	HOMO	Eg	I	A	μ
C_{36}– H_{12}	-----	–0.134, –0.229	------	–3.28	–4.17	0.89	-----	-----	5.71
Ni– C_{36}– H_{12}	0.570	–0.1437, –0.1308	------	–2.88	–4.04	1.15	-----	-----	0.71
$1H_2$– Ni– C_{36}– H_{12}	0.418	–0.120, –0.121	0.027, 0.016	–2.78	–4.24	1.45	-----	-----	2.20
$2H_2$– Ni– C_{36}– H_{12}	0.246	–0.288, –0.286	0.033, 0.073 0.073, 0.032	–2.53	–4.24	1.71	4.24	2.53	1.34
$3H_2$– Ni– C_{36}– H_{12}	0.244	–0.289, –0.286	0.0358, 0.0702 0.072, 0.0032 0.0002, 0.003	– 2. 54	–4.25	1.71	4.25	2.54	1.37
$4H_2$– Ni– C_{36}– H_{12}	0.249	–0.292, –0.290	0.033, 0.071 0.071, 0.033 0.021, –0.012 0.019, –0.02 0.0313, 0.073	–2.540	–4.25	1.71	----	----	1.53
$5H_2$– Ni– C_{36}– H_{12}	0.249	–0.293 –0.289	0.033, 0.023 –0.02, 0.072 0.019, –0.022 –0.001, 0.006	–2.545	–4.253	1.708	----	----	1.48

Table 3.

Structural and energetic parameters of the optimized nH_2 –Ni– C_{36}– H_{15}(n=1–4) (sheet) systems. All distances (d) are given in Å , energy $\Delta E_{ads.}$, in eV, calculated at the B3LYP/6–31G level of theory.

System	$\Delta E_{ads.}$	d(Ni–C)	d(C–C)	d(Ni–H)	d(H–H)	Wt%
C_{36}– H_{15}		–––––	1.40	––––––	––––––	
Ni– C_{36}– H_{15}	–6.365	1.824	1.412	–––––	––––––	
$1H_2$– C_{36}– H_{15}	–0.02	–––	–––	2.867, 3611	––––––	
$1H_2$– Ni– C_{36}– H_{15}	–0.655	1.8754	4.16	1.658, 1.659	0.811	
$2H_2$– Ni– C_{36}– H_{15}	–0.478	1.87474	1.417	1.6420, 2.442 3.177, 1.637	0.799, 0.764	
$3H_2$– Ni– C_{36}– H_{15}	–0.210	1.93597	1.42	1.690, 1.654 1.713, 1.789 1.729, 1.695	0.796, 0.811 0.791	3.97
$4H_2$– Ni– C_{36}– H_{15}	–0.174	1.874	1.418	2.464, 3.201 1.645, 1.647 3.988, 4.696 4.065, 4.803	0.745, 0.796 0.743, 0.743	

Table 4.

Natural bond orbital charges (Q) in au, HOMO, LUMO, and Eg energies in (eV), ionization potential (I/ eV), electron affinity (A/ eV) and dipole moment (μ) in Debye, for nH_2 –Ni– C_{36}– H_{15}(n=1–4) (sheet) systems.

System	Q_{Ni}	Q_C	QH	LUMO	HOMO	Eg	I	A	μ
C_{36}– H_{15}	––––	–0.1532	–––––	–2.91	–5.01	2.11	–––	–––	8.32
Ni– C_{36}– H_{15}	0.277	–0.127	–––––	–2.85	–4.95	2.12	–––	–––––	10.32
$1H_2$– Ni– C_{36}– H_{15}	0.272	–0.072	0.069, 0.045	–2.775	–4.88	2.11	–––	–––––	11.42
$2H_2$– Ni– C_{36}– H_{15}	0.256	–0.105	0.049, 0.051 –0.034, 0.023	–2.597	–4.49	1.89	–––	–––––	10.15
$3H_2$– Ni– C_{36}– H_{15}	0.110	–0.072	0.048, 0.031 0.063, 0.022 0.039, 0.0357	–2.68	–4.45	1.77	4.45	2.68	12.23
$4H_2$– Ni– C_{36}– H_{15}	0.251	–0.110	0.049, 0.049 –0.033, 0.025 0.0026, 0.002 –0.004, 0.008	–2.74	4.483	1.75	4.48	2.74	12.01

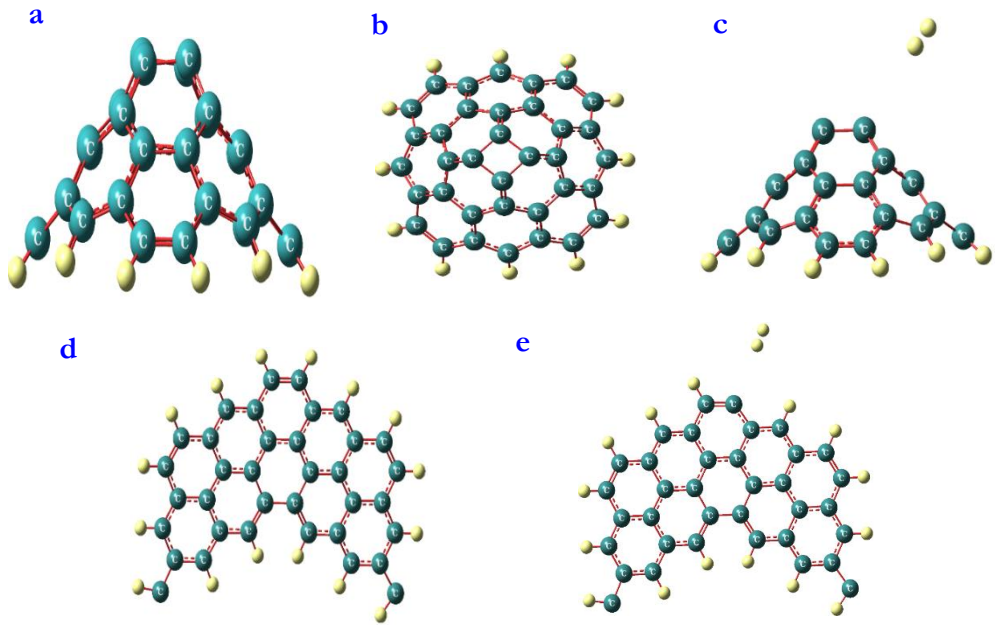

Fig.1: (**a**, **b**) **Side view top view of carbon nanocones** ($C_{36}H_{12}$), **with disclination angle 120º and a rhombohedral tip**, (**c**) **optimized geometries of** $1H_2$–$C_{36}H_{12}$, (**d**, **e**) **optimized geometries of Carbon nanocone sheet** ($C_{36}H_{15}$) **and** $1H_2$–$C_{36}H_{15}$. **Carbon**, **Hydrogen atom is shown in teal and yellow respectively**.

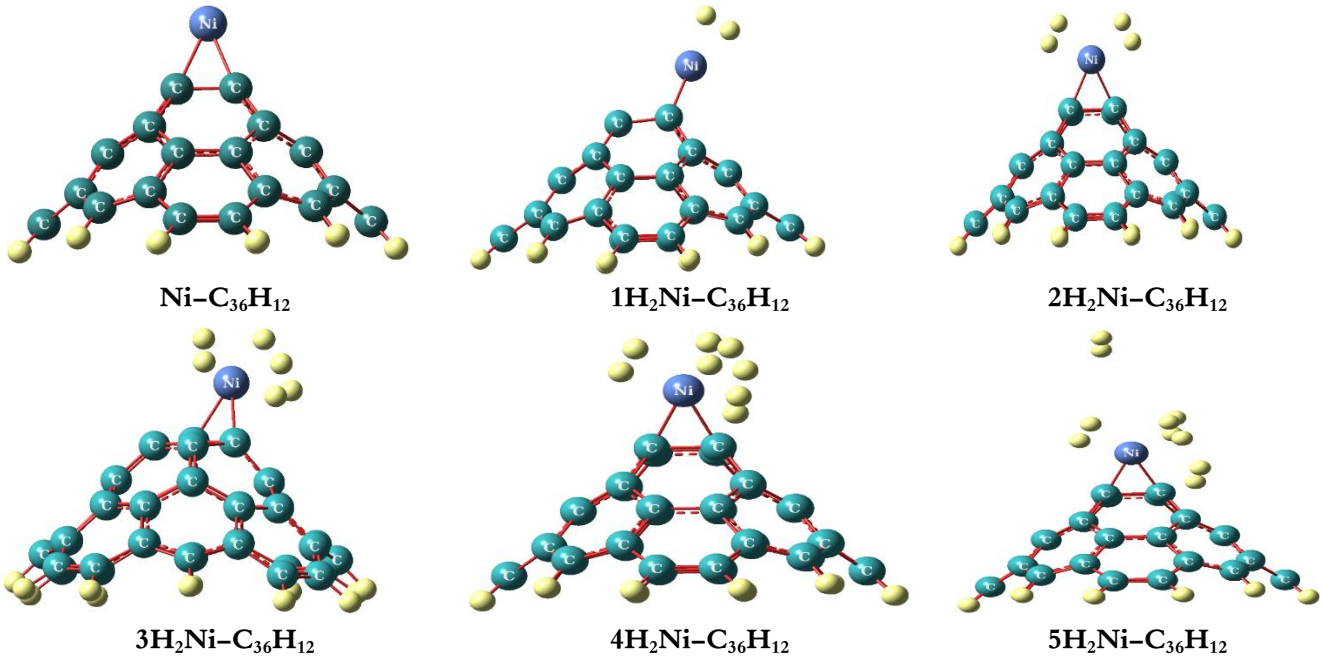

Fig. 2: **The optimized geometries of** $Ni–C_{36}H_{12}$ **and** nH_2–Ni– $C_{36}H_{12}$ (n = 1–5) **nanocone complexes**. **Carbon**, **nickel**, **and hydrogen atom is shown in teal**, **blue**, **and yellow respectively**.

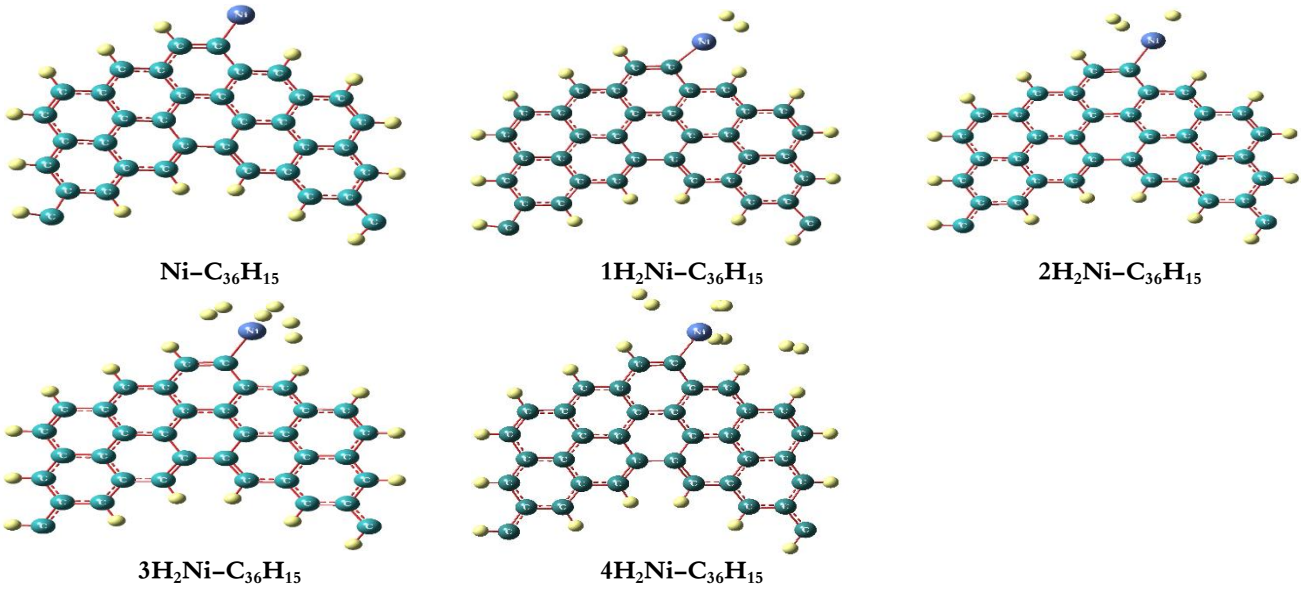

Fig. 3: The optimized geometries of $Ni–C_{36}H_{15}$, $nH_2–Ni–C_{36}H_{15}$ (n = 1–4) nanocone sheet complexes. Carbon, Nickel, and Hydrogen atom is shown in teal, blue, and yellow, respectively.

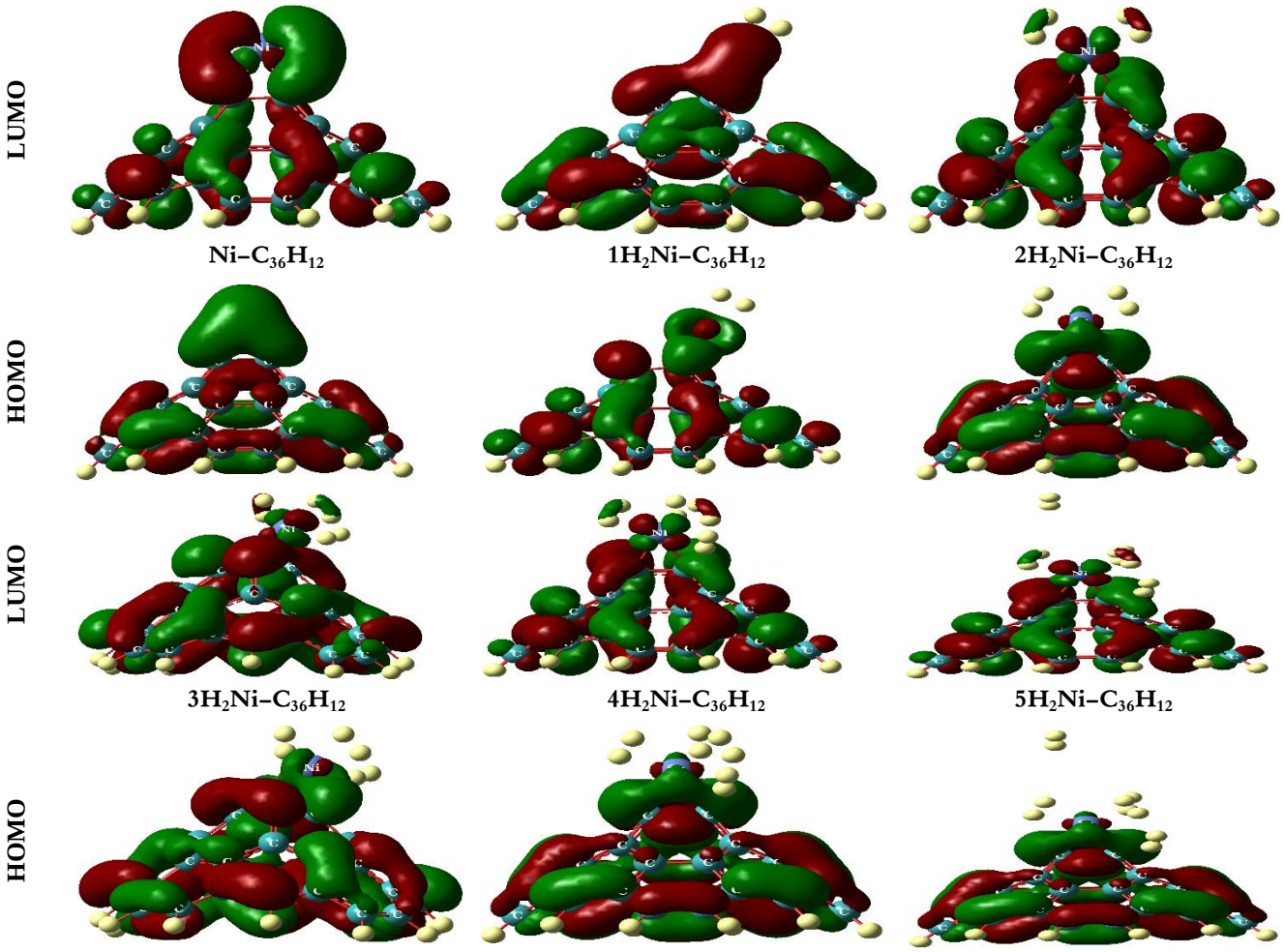

Fig. 4: Frontier orbital isosurface plots of $Ni–C_{36}H_{12}$ and $nH_2Ni–C_{36}H_{12}$ (n=1–5) complexes (at isovalue . 02).

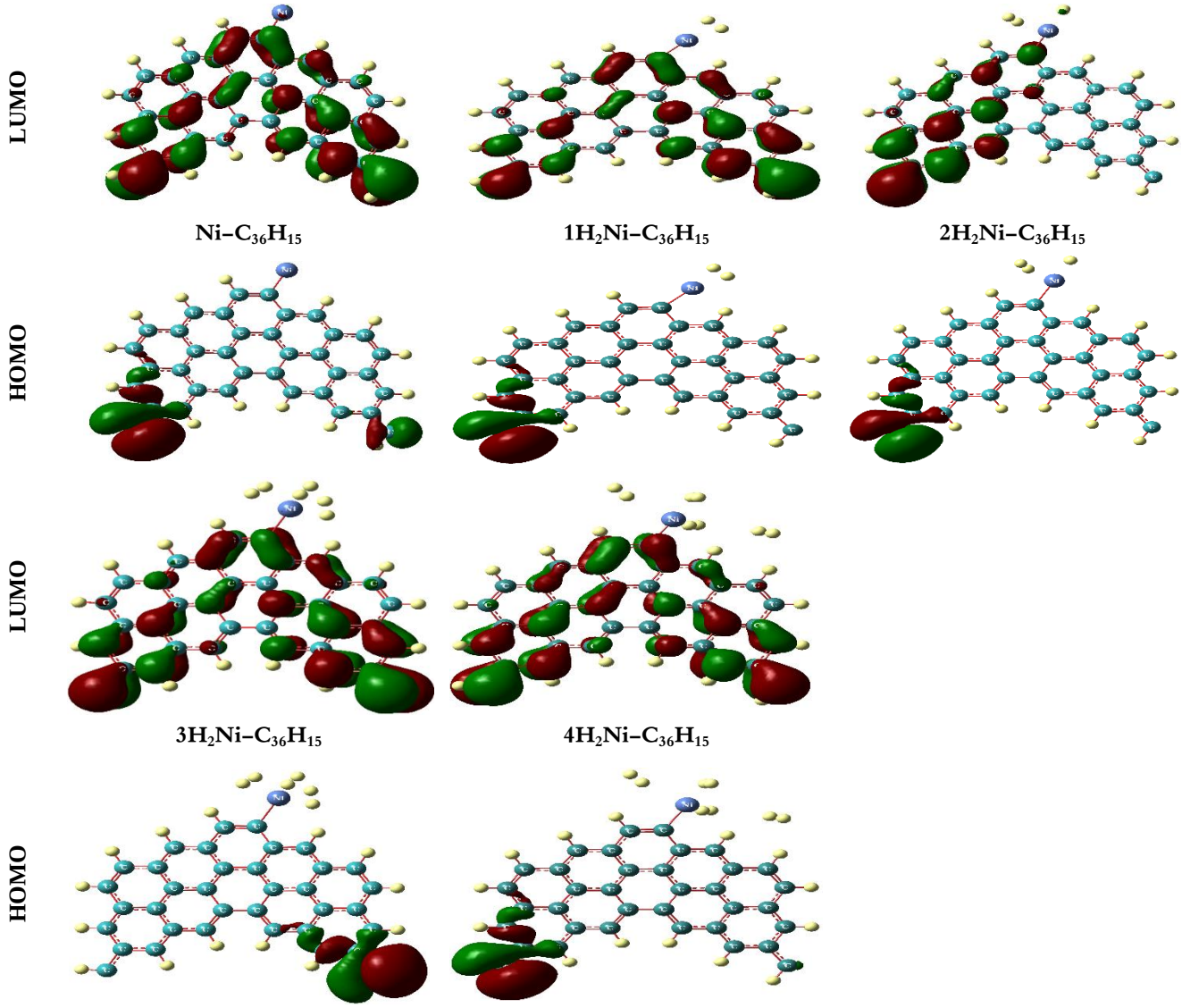

Fig. 5: **Frontier orbital isosurface plots of $Ni–C_{36}H_{15}$ and $nH_2Ni–C_{36}H_{15}$ (n=1–4) complexes (at isovalue 0.02).**

4. Interpretation of Results

4.1. Interaction of Ni on NC and CNCS :

We have first considered the structure of CNC and CNCS with a disclination angle of 120° and height of 5 Å ,containing 36 carbon atoms, the relaxed structures, using DFT are illustrated in Figure 1(a, b, d). To reduce boundary effects, the CNC and CNCS were hydrogen–saturated at the ends. a single H_2 molecule interacts with $C_{36}H_{12}$ NC and $C_{36}H_{15}$ NCS was computed, and the adsorption energy was determined by optimizing a single molecule of H_2 on the CNC and CNCS surface, and defined as:

$$\Delta E_{ads}(H_2) = E_{total}(\text{substrate}) \text{ with } (H_2) - E_{total}(\text{substrate}) - E_{total}(\text{single } H_2) \quad (1)$$

For $C_{36}H_{12}$ NC and $C_{36}H_{15}$ NCS, the adsorption energy is –0.008 and –0.02 eV, this is in the very weak physisorption range, which is out of the range of -0.2 to -0.6 eV as stated by DoE and possesses long equilibrium distances of hydroen–surface $(\sim 4.23\ \text{Å}), (\sim 3.61\ \text{Å})$ Figure 1(c,e). The decorated $Ni - CNC$ and $Ni - CNCS$ effect on adsorption of H_2 enhancement was verified. Therefore, we examine the interaction between Ni and ($C_{36}H_{12}$ NC and $C_{36}H_{15}$ NCS). We have adsorbed a single atom of Ni on the optimization $C_{36}H_{12}$ NC and $C_{36}H_{15}$ NCS at about ~ 1.9 Å from the surface and for each, full optimization of geometry is carried out. Figures 2, 3 show the obtained configurations. To determine the configuration stability, the following expression was used to compute the adsorption energies:

$$\Delta E_{ads} = E(Ni + (CNC \text{ or } CNCS)) - E(CNC \text{ or } CNCS) - E(Ni), \quad (2)$$

where $E(Ni + (CNC \text{ or } CNCS))$, $E(Ni)$ and $E(CNC \text{ or } CNCS)$ ar , respectively, the doped ($Ni - C_{36}H_{12}$ and $Ni - C_{36}H_{15}$), isolated Ni atom and $C_{36}H_{12}$ and $C_{36}H_{15}$ energies. The adsorption energies computed at $B3LYP/6 - 31G\,(d,p)$, the most stable geometries for ($Ni - C_{36}H_{12}$ and $Ni - C_{36}H_{15}$) are displayed in Figures 2, 3. Tables 1–4, summarize the predicted binding energies and structural quantities for the best cases. Adsorption energies were found to be –4.13 and –6.365 eV for $Ni - C_{36}H_{12}$ and $Ni - C_{36}H_{15}$, respectively. We point out that the negativity of adsorption energies illustrates that the adsorption is energetically promising and is much larger than ΔE_{ads} of the H_2.

Adsorption energies signify that the adsorption is energetically favored and are much greater than the average H_2 $(-0.20, \text{and} -0.60\ \text{eV})$ energies, to ensure $Ni - C_{36}H_{12}$ and $Ni - C_{36}H_{15}$ complexes stability if the H_2 molecules are released. These optimized $Ni - C_{36}H_{12}$ and $Ni -$

$C_{36}H_{15}$ are used to add hydrogen molecules to the doped Ni. As shown in Table 4, concerning $Ni-C_{36}H_{15}$, the resulting dipole moments of 10.32 Debye, compared to, 8.32 Debye for $C_{36}H_{15}$ to improve the interaction of Van der Waals between $C_{36}H_{15}$ and H_2. The HOMO and the LUMO frontier orbitals play a significant role in the chemical reaction of reactant molecules.; thus, the analysis of the frontier orbitals of $Ni-C_{36}H_{12}$ and $Ni-C_{36}H_{15}$ is necessary. It can be seen that in Tables 2, 4, HOMO levels of $Ni-C_{36}H_{12}$ and $Ni-C_{36}H_{15}$ are nearly unchanged compared with those of pure pristine $C_{36}H_{12}$ and $C_{36}H_{15}$. LUMO levels for $Ni-C_{36}H_{12}$ is decreased but for $C_{36}H_{15}$ remain unchanged. The HOMO–LUMO energy gap of $Ni-C_{36}H_{12}$ and $Ni-C_{36}H_{15}$ were found to be (1.15 and 2.12 eV). Figures 4, 5 illustrate the HOMO and LUMO distributions for $Ni-C_{36}H_{12}$ and $Ni-C_{36}H_{15}$, the frontier orbital analysis for $Ni-C_{36}H_{12}$ and $Ni-C_{36}H_{15}$ indicates the transfer of electrons to $C_{36}H_{12}$ and $C_{36}H_{15}$. From analysis NBO, the Ni charge is $0.570(C_{36}H_{12})$, $0.277(C_{36}H_{15})$, while on the nearest neighbor C is $-0.1437, -0.1308$ $(C_{36}H_{12})$ and -0.127 $(C_{36}H_{15})$ These results indicate the transfer of electrons from the Ni atom to the neighbors C, where the overlap of Ni–d orbitals with (sp C) orbitals for bonds of (Ni– C). This transfer of charge increases the H_2 molecule uptake.

4.2. Interaction of nH_2 with [Ni + CNC] and [Ni + CNCS] :

In this section, we study the ΔE_{ads} of adsorbed hydrogen molecules on $Ni-C_{36}H_{12}$ and $Ni-C_{36}H_{15}$. The H_2 average adsorption energy over $Ni-C_{36}H_{12}$ and $Ni-C_{36}H_{15}$ is defined as:

$$\Delta E_{ads}(H_2) = [E(nH_2 + (Ni + CNC \text{ or } CNCS) - E(nH_2) - E(Ni + CNC \text{ or } CNCS)]/n \quad (3)$$

$E(nH_2 + (Ni + CNC \text{ or } CNCS))$ is fully relaxed $nH_2 + (Ni + CNC \text{ or } CNCS$ total energy, $E(nH_2)$ is hydrogen molecules energy, $E(Ni + CNC \text{ or } CNCS)$ is the $Ni +$ CNC or CNCS total energy, and (n) is the hydrogen molecules number. Exothermic adsorption is related to the negative value of $\Delta E_{ads}(H_2)$.

The optimal geometries of nH_2–Ni–CNC (n=1–5), and nH_2–Ni–CNCS (n=1–4) are illustrated in Figures 2, 3. These results present a detailed analysis of the structural and energetic parameters of various $nH_2Ni-C_{36}H_{12}$ and $nH_2Ni-C_{36}H_{15}$ complexes. The complexes are optimized using density functional theory at the B3LYP/6–31G level of theory. The study investigates the effects of adding up to 5 hydrogen molecules on the structural and energetic properties of these complexes. The results show that the addition

of H_2 molecules leads to significant changes in the geometries, energies, and electronic properties of the complexes.

4.2.1 Adsorption Energies:

The Ni–CNC was found to adsorb up to five hydrogen molecules ΔE_{ads} are (–0.813, –0.847,–0.573,–0.42, and –0.343 eV) for nH_2–Ni–CNC (n=1–5), respectively as shown in Table 1, whereas the Ni–CNCS was found to adsorb four hydrogen molecules ΔE_{ads} are (–0.655,–0.478 ,–0.210, and –0.174) for nH_2–Ni–CNCS (n=1–4), respectively as illustrated in Table 3. These results indicate that ΔE_{ads} of nH_2–Ni–CNC (n=3–5), are within the DOE–defined range $(\sim -0.2 \text{ to } -0.6 \text{ eV})$ and ΔE_{ads} of nH_2–Ni–CNCS (n=2,3), are also in window, seem to be optimal for use in fuel cell based on the storage capacity investigation.

4.2.2 HOMO–LUMO band gap

The Ni–CNC structures were found to adsorb up to five hydrogen molecules, and have band gap (Eg) values that are (1.45,1.71, 1.71, 1.71, and 1.71 eV), respectively, as shown in Table 2. As indicated in Table 4, the Ni–CNCS structures were found to adsorb four hydrogen molecules, and have Eg values that are (2.107 ,1.89 ,1.77 ,and 1.7 eV) respectively. The lowered HOMO–LUMO gap. according to these findings, materials' ability to store hydrogen can be affected in some ways by narrowing the band gap between their lowest unoccupied molecular orbital (LUMO) and highest occupied molecular orbital (HOMO). This indicates the electronic stability and reactivity of the complexes. Figures 4, 5 illustrate the HOMO and LUMO distributions for $Ni - C_{36}H_{12}$ and $Ni - C_{36}H_{15}$, the frontier orbital analysis for $Ni - C_{36}H_{12}$ and $Ni - C_{36}H_{15}$ indicates the transfer of electrons to $C_{36}H_{12}$ and $C_{36}H_{15}$.

The potential of ionization (IP) and electron affinity (EA) were computed from HOMO, and LUMO energies by using the approximation of Koopmans, where IP = –HOMO and EA= –LUMO. (IP) and (EA) for revirsable and irreversible interactions are given in Tables 2,4

4.2.3 The effects of hydrogen adsorption on some properties:

4.2.3.1 Electronic Properties:

according to the natural bond orbital (NBO) population (A. E. Read, 1983,4066–A. E. Read,1988, 899). The natural bond order charges provide insights into the electronic distribution within the complexes. The charge distribution changes with the introduction of H2 molecules, reflecting the altered bonding interactions and charge transfer between the metal center and the ligands.

The charge on Ni in $(nH_2C_{36}H_{12})$(n=1–5) in Table 2 ranges from(0.244 to 0.418 a.u) and on

the nearest neighbor carbons are (–0.121 and –0.292 a.u)

In sheet ($nH_2C_{36}H_{15}$)(n=1–4) indicated from Table 4, the charge on Ni ranges from (0.11 to 0.272 a.u), and on the nearest neighbor carbon are (–0.11 and –0.072 a.u). This indicates that Ni donates electrons to the neighboring C atoms on CNC where the d– orbitals of Ni atom overlap with the sp orbitals of the Ni–C bonds to form the mixed spd hybridization. This transfer of charge increases the H_2 molecules' uptake.

Researchers can obtain a greater understanding of the structure–property links in these complexes by analyzing the results and investigating their possible applications in a variety of disciplines.

4.2.4 The Hydrogen Storage Capacity (wt %):

The relation was used to compute the gravimetric hydrogen storage capacity, which is the amount of hydrogen stored per unit mass of material.

$$Wt\% = \frac{nlM_{H2}}{nlM_{H2}+lM_{Ni}+mM_C} X\ 100 \quad (4)$$

where n: number of H_2 molecules adsorbed on each Ni atom, l: number of Ni atoms, m: number of carbon atoms, and M: the atomic or molecular weight. For the complexes $nH_2 + Ni_2–C_{36}$ (n = 10, 6), the hydrogen storage capacities are expected to be 5.05 and 3.97% CNC, CNCS, respectively. To maximize the storage capacity of H_2, metal clustering must be avoided.

5. Conclusion

The study investigates the hydrogen storage capabilities of Ni Functionalized CNCs and CNCSs using Density Functional Theory calculations. Results show the physisor'tion of hydrogen storage reactions meet DOE targets for practical applications. The studied systems may provide guidelines for the development of solid–state hydrogen storage materials. The goal is to optimize current hydrogen storage technologies, and search for new hydrogen storage materials with specific properties. Two types of reactions, namely reversible and irreversible are found. While the desorption activation Barriers of the complexes nH2–Ni–CNC (n=3–5) are –0.573, –0.427 and –0.343 respectively, and nH2–Ni–CNCS (n =2,3) – 0.478 and –0.24 are inside the Department of Energy domain (–0.2 to –0.6 eV). The complexes nH2–Ni–CNC (n=1,2) –0.813, –0.847 and nH2–Ni–CNCS (n =1,4) – 0.655 and –0.17 are outside. The results imply that these materials' advantageous structural and energetic qualities make them promise for use in hydrogen storage applications.Consequently, discovering materials that exhibit all of the unique

attributes required for hydrogen storage remains a challenge for materials research. We hope that present calculations suggest an approach to characterize and engineer new nanostructured materials as potential power sources.

References and sources:

[1]– M. Mohsin, H. W. Kamran, M. A. Nawaz, M. S. Hussain and AS (2021). Dahri, Assessing the impact of transition from nonrenewable to renewable energy consumption on economic growth–environmental nexus from developing Asian economies,Journal of Environmental Management,111999, Volume 284.
https://doi.org/10.1016/j.jenvman.2021.111999

[2]– B. Modu, Md . P. Abdullah, A. L Bukar and M. F. Hamza,2023
A systematic review of hybrid renewable energy systems with hydrogen storage: Sizing, optimization, and energy management strategy, International Journal of Hydrogen Energy, Volume 48, Issue 97, Pages 38354–38373, ISSN 0360–3199,
https://doi.org/10.1016/j.ijhydene.2023.06.126

[3]– Züttel A. (2004)Hydrogen storage methods. Naturwissenschaften. Apr;91(4):72–157. Mar 17. PMID: 15085273.
Doi: 10.1007/s00114–004–0516–x
.

[4] A.C. Dillon, K.M. Jones, T.A. Bekkedahl, C.H. Kiang, D.S. Bethune,M.J. Heben, Nature 386 (1997)Storage of hydrogen in single–walled carbon nanotubes 377–379
http://dx.doi.org/10.1038/386377a0 .

[5]– A. Kose, N. Yuksel, M. F. Fellah , (2022)Hydrogen adsorption on Ni doped carbon nanocone, volume 124,108921,ISSN 0925–9635,
https://doi.org/10.1016/j.diamond.2022.108921

[6]– S. Abdel Aal, A. S. Shalabi, K. A. Soliman.(2015), "High Capacity Hydrogen Storage in Ni Decorated Carbon Nanocone: A First–Principles Study", Journal of Quantum Information Science, Vol.5 No.4,
DOI: 10.4236/jqis.2015.54016

[7]– A. S. Shalabi , A. M. El Mahdy and H. O. Taha ,A first principles study ,17 November 2012 ,J Mol Model (2013),The effect of C–vacancy on hydrogen storage and characterization of H2 modes on Ti functionalized C_{60} fullerene 19:1211–1225 ,
DOI 10.1007/s00894–012–1615–9

[8]– A.S. Shalabi, A.M. El Mahdy, K.A. Soliman and H.O. Taha ,2014, Theoretical characterisation of irreversible and reversible hydrogen storage reactions on Ni–doped C6o. Molecular Physics.
DOI: 10 1080/00268976.2014. 928754

[9]– A.S. Shalabi, K. A. Soliman and H. O. Taha ,2014,A comparative theoretical study of

metal Functionalized carbon nanocones and carbon Nanocone sheets as potential hydrogen Storage materials .
DOI: https://doi.org/10.1039/C4CP02726D .
[10]– Xu H, Ni K, Li X–K, Zhu S and Fan G–H, 2017, First–principles study of CO catalytic oxidation on Pd–doped single wall boron nitride nanotube Comput. Theor. Chem. 1115 37–44
[11]– K. Tomson, C. Wongchoosuk, 2019, "Inkjet printing of room–temperature gas sensors for identification of formalin contamination in squids", J. Mater. Sci. Mater. Electron., 30, 4782.
https://doi.org/10.1007/s10854–019–00772–9
[12] – H. Soleymanabadi, J. Kakemam, Phys. E. 2013, "A DFT study of H2 adsorption on functionalized carbon nanotubes" , 54, 115.
https://doi.org/10.1016/j.physe.2013.06.015
[13]– A. D. Becke, 1993, " Density-functional thermochemistry. III. The role of exact exchange" , J. Chem. Phys., 98, 5648.
https://doi.org/10.1063/1.464913
[14] – S. H. Vosko, L. Wilk, M. Nusair, Can. J. Phys. 1980, " Accurate Spin–Dependent Electron Liquid Correlation Energies for Local Spin Density Calculations: A Critical Analysis" , 58, 1200.
http://dx.doi.org/10.1139/p80–159
[15]– A. D. Becke, Phys. Rev. 1988, "Density–functional exchange–energy approximation with correct asymptotic behavior" , 38, 3098.
Doi: 10.1103/physreva.38.3098
[16]– C. Lee, W. Yang, R. G. Parr, 1988, Phys. Rev. B, " Development of the Colle–Salvetti correlation–energy formula into a functional of the electron density" , 37, 785.
https://doi.org/10.1103/PhysRevB.37.785
[17[– R. L. Martin, F. Illas, Phys. Rev. Lett. 1997, "Antiferromagnetic Exchange Interactions from Hybrid Density Functional Theory" ,79, 1539.
[18]– I. P. R. de Moreira, F. Illas, R. L. Martin, 2002, "Accurate density functionals: Approaches using the adiabatic– connection fluctuation– dissipation theorem" , Phys. Rev. B, 65, 235109
DOI:https://doi.org/10.1103/PhysRevB.65.235109
[19] C. Wolverton, D.J Siegel, A.R. Akbarzadeh, V. Ozoliņš, 2008, "Discovery of novel hydrogen storage materials: an atomic scale computational approach", J. Phys. Condens. Matter 20, 064228.
https://doi.org/10.1088/0953–8984/20/6/064228
[20] M.J. Frisch, et al., Gaussian 09, Revision D.01 (Gaussian, Inc., Wallingford, CT,2010)
[21] A. E. Read, F. Weinhold, "Natural bond orbital analysis of near–Hartree–Fock water dimer", J. Chem. Phys., 78(1983)4066.
https://doi.org/10.1063/1.445134
[22] J. E. Carpenter, F. Weinhold, 1988, "Analysis of the geometry of the hydroxymethyl radical by the "different hybrids for different spins" natural bond

orbital procedure, **J**. **Mol**. **Struc**. **THEOCHEM**, 169,41. https://doi.org/10.1016/0166–1280(88)80248–3.

[23] A. **E**. **Read**, **L**. **A**. **F**. **Weinhold**, 1988, "**Intermolecular interactions from a natural bond orbital**, **donor– acceptor viewpoint**", **Chem**. **Rev**., 88,899. https://doi.org/ 10.1021/cr00088a005.